Response to reviewer #2' comments

We thank the reviewer for the time and effort in conducting a thorough review of our manuscript. The constructive comments and valuable suggestions have substantially improved the quality of this paper. Below is our point-by-point response to all the comments. The reviewer's comments are presented in *Italics*, followed by our corresponding responses marked in blue and all revisions made to the manuscript highlighted in red.

Major Comments

Throughout the manuscript, the authors discuss the performance of the CRACMM mechanism using various statistical metrics. However, in many cases the discussion lacks reference to relevant previous work that would help contextualize these results. In addition, statements such as "performance is good in Region 1" or "performance is moderate in Region 2" are presented without further interpretation. I encourage the authors to not only report these findings but also provide explanations for the such differences in performance, ideally supported by literature and known chemical mechanisms and meteorological factors, using additional figures/tables.

Thanks for the constructive comment. We agree that model performance metrics alone are insufficient without appropriate context and interpretation. In response, we have revised the manuscript to strengthen the discussion of CRACMM performance by explicitly comparing our results with relevant previous studies, detailed revisions are shown blow, and we believe they substantially improve the interpretability and robustness of the model evaluation.

(1) Added references to compare with previous work.

Lines 431-438: Previous studies have reported similar R values. For example, the evaluation results of $PM_{2.5}$ simulations using CMAQ over five key regions in China，which is consistent with the regions considered in this study, showed that the R were generally below 0.6 in July (Huang et al., 2024). In addition, a multi-model intercomparison study involving CAMx6.2, CAMx7.1, CMAQv5.0.2 and CMAQv5.3.2 reported R values of 0.58, 0.55, 0.60, and 0.39, respectively, for mean $PM_{2.5}$ concentrations in China during 2014–2017. The CAMx6.2, CAMx7.1, and CMAQv5.0.2 simulations covered the entire country, whereas CMAQv5.3.2 was evaluated over eastern China (Meng et al., 2026).

(2) Added some references as explanations for the performance.

Lines 361 to 367: The strong influence of temperature and solar radiation on photochemical processes during summer may result in more pronounced diurnal variations in chemical composition, making the simulation of chemical processes more challenging (Seinfeld et al., 1998). Moreover, the chemical mechanisms may inadequately capture non-linear interactions

and the influence of SOA (Harrison et al., 2022), further reducing the correlation. Additionally, synoptic-scale variations can also affect the spatial distribution and concentration of key atmospheric species (Zhu et al., 2023).

(3) In order to strengthen these interpretations, evaluation of temperature, relative humidity, and wind speed are added (Tables S11–S13) (shown below) to illustrate the role of meteorological factors. Please refer to below revisions.

Lines 396-400: For July, larger discrepancies are likely associated with more complex meteorological conditions, as reflected by the relatively poor performance of wind speed, particularly in the SCB region. In contrast, the simulation performance of relative humidity and temperature shows only minor differences relative to the other three months (Tables S11–S13).

Table S11 Evaluation of WRF-simulated temperature over five regions

Month	Region	R	NMB	MB	RMSE	OBS-ave	SIM-ave
January	BTH	0.9	27.8	-2.0	2.9	-3.9	-5.9
	FWP	0.9	-13.5	-1.2	2.3	0.2	-1.0
	PRD	0.9	-4.6	-0.7	2.1	14.3	13.7
	SCB	0.9	11.3	-0.8	2.3	5.7	5.0
	YRD	1.0	-41.3	-1.8	2.4	4.6	2.9
April	BTH	0.8	-4.9	0.5	2.1	14.1	13.5
	FWP	0.9	-0.1	0.0	2.0	13.6	13.6
	PRD	0.7	6.6	1.6	2.5	23.9	25.5
	SCB	0.8	-3.7	-0.2	2.7	16.6	16.5
	YRD	0.8	0.3	-0.1	1.9	16.1	16.0
July	BTH	0.7	5.8	1.6	3.4	26.4	28.0
	FWP	0.7	8.2	2.2	4.3	26.3	28.4
	PRD	0.7	5.0	1.5	3.0	29.6	31.1
	SCB	0.5	-1.2	-0.1	3.8	25.9	25.8
	YRD	0.6	-1.5	-0.5	3.0	28.2	27.6
October	BTH	0.8	7.2	0.8	2.5	12.1	12.9
	FWP	0.5	10.6	1.2	4.9	11.2	12.4
	PRD	0.3	18.6	3.9	8.6	21.2	25.1
	SCB	0.6	1.1	0.4	5.2	14.7	15.0
	YRD	0.9	-0.9	-0.3	2.0	19.1	18.8

Table S12 Evaluation of WRF-simulated relative humidity over five regions

Month	Region	R	NMB	MB	RMSE	OBS-ave	SIM-ave
January	BTH	0.8	-10.0	-4.3	12.3	44.4	40.1
	FWP	0.6	-3.6	-2.0	12.9	37.0	35.0
	PRD	0.7	-25.3	-14.4	19.1	55.5	41.2
	SCB	0.4	17.0	-7.8	26.0	65.1	57.3
	YRD	0.9	-10.2	-6.6	12.7	63.6	57.0
April	BTH	0.8	-18.9	-9.0	19.9	45.4	36.3
	FWP	0.9	-20.7	-13.0	17.4	60.2	47.2
	PRD	0.5	-16.9	-13.0	16.6	76.5	63.5
	SCB	0.6	-4.6	-5.8	15.5	72.6	66.9
	YRD	0.7	-12.1	-8.8	16.4	72.3	63.5
July	BTH	0.7	-16.8	-13.1	19.2	78.5	65.4
	FWP	0.5	-27.7	-19.7	26.6	69.9	50.2
	PRD	0.7	-12.7	-9.9	16.0	77.0	67.1
	SCB	0.4	-4.3	-3.7	17.9	77.5	73.8
	YRD	0.7	-1.3	-1.2	11.6	81.3	80.0
October	BTH	0.7	-18.7	-12.6	20.9	62.8	50.3
	FWP	0.2	-8.8	-6.2	27.6	68.4	62.3
	PRD	0.3	-6.8	-4.8	25.2	69.4	64.6
	SCB	0.3	8.5	5.2	30.5	73.8	79.0
	YRD	0.7	-6.9	-5.3	10.3	76.7	71.4

Table S13 Evaluation of WRF-simulated wind speed over five regions

Month	Region	R	NMB	MB	RMSE	OBS-ave	SIM-ave
January	BTH	0.8	43.6	1.0	1.6	2.6	3.6
	FWP	0.6	20.1	0.3	1.1	2.6	2.9
	PRD	0.8	61.0	1.5	1.8	2.6	4.1
	SCB	0.4	178.7	0.9	1.3	1.6	2.5
	YRD	0.7	40.5	0.8	1.4	3.0	3.8
April	BTH	0.6	12.5	1.8	7.3	2.3	4.1
	FWP	0.6	21.9	0.4	1.4	3.1	3.5
	PRD	0.3	46.1	0.9	1.4	2.4	3.3
	SCB	0.5	50.1	0.8	1.3	2.1	2.9
	YRD	0.6	40.2	0.8	1.5	3.1	3.9
July	BTH	0.2	-34.0	5.9	145.4	-2.9	3.1
	FWP	0.2	14.8	0.2	2.2	2.6	2.8
	PRD	0.4	15.9	0.4	1.9	2.8	3.2
	SCB	0.1	-0.8	-0.1	1.6	1.9	1.9
	YRD	0.5	34.3	0.9	2.6	3.8	4.7
October	BTH	0.7	62.4	1.0	1.5	2.0	3.0
	FWP	0.3	28.9	0.3	1.3	2.0	2.3
	PRD	0.3	65.1	1.8	2.8	3.1	4.9

SCB	0.2	58.9	0.7	1.4	1.5	2.2
YRD	0.8	47.1	1.0	1.6	2.9	3.8

(4) We have revised the text as follows to illustrate why $PM_{2.5}$ concentrations in July is low with two additional figures, Figure S5 and Figure S6.

Lines 334-338: This decline is mainly attributable to the increased precipitation which washed out pollutants, in the southern and eastern parts of China compared to other months (Figure S5). In addition, higher planetary boundary layer (PBL) heights during the warm season in the south, particularly in the YRD region of China, than other months (Figure S6), enhancing atmospheric mixing and dilution, and led to the decrease in $PM_{2.5}$ concentrations.

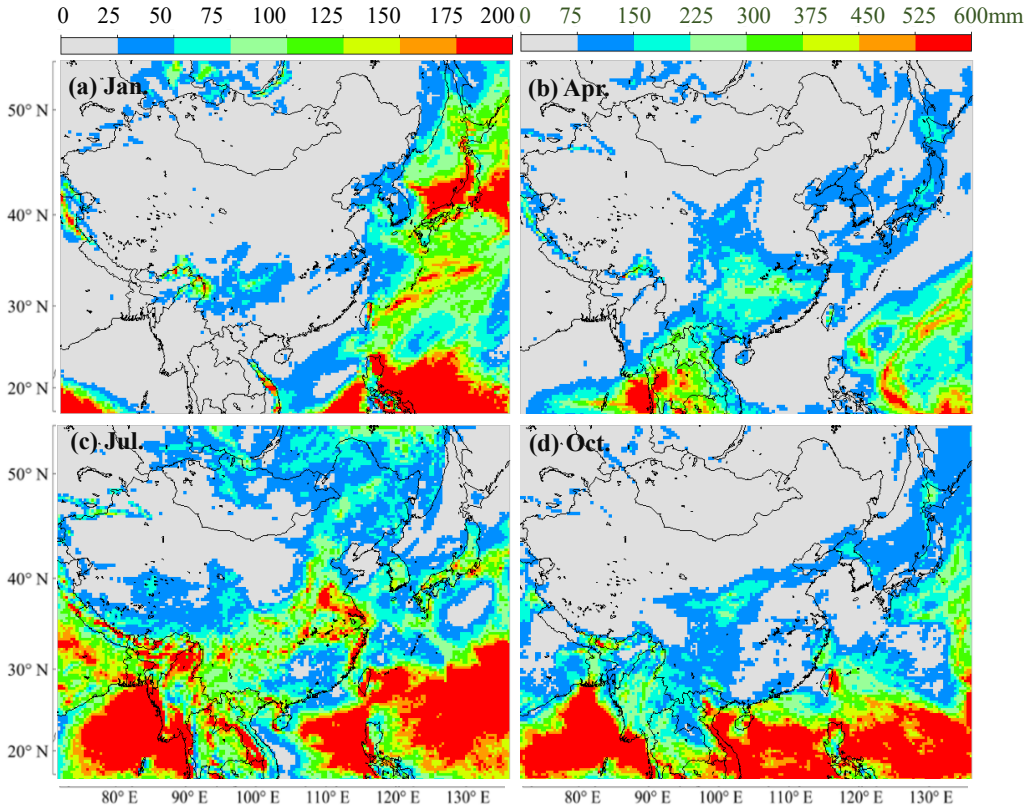

Figure S5 Spatial distribution of monthly total precipitation (mm). Note: Panels (a), (b), and (d) share a common color bar (top left), whereas panel (c) uses a separate color bar (top right) to better highlight spatial variations

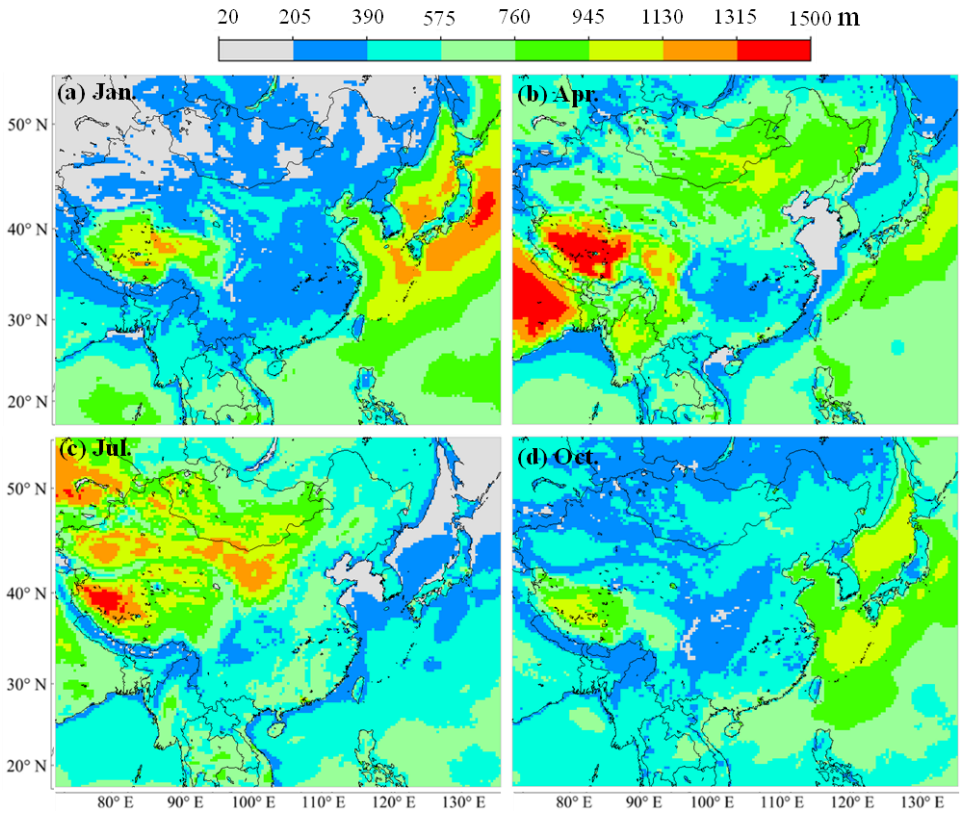

Figure S6 Spatial distribution of monthly mean PBL height (m).

It is my opinion that the introduction section consists of somewhat detailed description of the different chemical mechanisms. I would encourage the authors to move some of the text to a description section or to the supplement and focus more on the motivation of this work. Possible improvements could include: (a) discussing existing literature on air quality modeling over China (b) the region-specific limitations of using a (relatively) simpler (or older) chemical mechanism (c) any computational cost related arguments (d) possible usage of complicated chemistry schemes in other regional scale models (e) potential to use an advanced chemical mechanism in global models (with an advancement in high performance computing).

Below, we provide point-by-point responses to the comments.

(a) discussing existing literature on air quality modeling over China

We have expanded the introduction and discussion sections to include relevant studies on air quality modeling over China. In particular, those studies discuss recent applications of CMAQ and CAMx models, and their performance in simulating $PM_{2.5}$ and secondary aerosol formation. Relevant references have been added to highlight key findings, which provide context for our study. Below are revisions in the main text.

Lines 49-72:

Chemical transport models such as the Community Multiscale Air Quality (CMAQ) model (Byun and Schere, 2006) have been widely applied in China to investigate air quality issues, including seasonal $PM_{2.5}$ and ozone distributions and their formation mechanisms. The CMAQ version 5.02 and 5.3.2, both versions are equipped with the gas-phase mechanism of State Air

Pollution Research Center version99 (Saprc99) and Carbon Bond 6 version (CB6). These two chemical mechanisms were employed to simulate air quality over China during 2013–2019 (Mao et al., 2022). In that study, $PM_{2.5}$ were examined in the North China Plain (NCP), Yangtze River Delta (YRD), and Pearl River Delta (PRD), while it was overestimated in the Chengyu Basin (CY) and Fen-Wei Plain (FWP) regions with NMB and NME values greatly exceeded the suggested criteria. In addition, the FWP and CY also showed lower R than the benchmark ($R<0.4$) suggested by Emery et al during heavy polluted episode (Emery et al., 2017). During 2014–2017, the Comprehensive Air Quality Model with Extension (CAMx) (Yarwood et al., 2007) version 6.2, version 7.1, CMAQv5.0.2, and CMAQv5.3.2 models performed quite well in $PM_{2.5}$ mean performance. The bias and error terms of the four models were resemblant small: −0.29, −0.07, −0.04, and −0.11 for NMB and 0.51, 0.48, 0.53, and 0.52 for NME, 0.58, 0.55, 0.60, and 0.39, for R respectively (Meng et al., 2026), the CAMx6.2, CAMx7.1, and CMAQv5.0.2 simulations covered the entire country, whereas CMAQv5.3.2 was evaluated over eastern China. (Meng et al., 2026). According to Kang et al's research, the model shows good performance for $PM_{2.5}$ in most areas, except for the PRD region, where the mean fractional biases (MFB) for $PM_{2.5}$ using Saprc serious mechanisms are slightly outside the recommended range (Boylan and Russell, 2006). According to Huang's research, evaluation results of $PM_{2.5}$ simulation by SOAP3 in CAMx in BTH, YRD, PRD, FWP, SCB and PRD areas, the R values are 0.31, 0.45, 0.38, 0.48, and 0.15 in July, respectively. In November, the R values are also low for PRD and FWP, 0.30 and 0.48, respectively (Huang et al., 2024).

(b) the region-specific limitations of using a (relatively) simpler (or older) chemical mechanism
We have added a discussion on region-specific limitations of using a relatively simpler or older chemical mechanism in the manuscript.

Lines 73-150: Existing studies indicate that different chemical mechanisms vary significantly in terms of the number of species, reaction complexity, and the coverage of chemical pathways, could lead to noticeable differences in regional air quality model performance. With this realization, we further examined the limitations of the commonly used chemical mechanisms (CB, Saprc and Regional Atmospheric Chemical Mechanism (RACM)). In CB mechanism, model species represent the concentrations of constituent groups regardless of the molecule to which they are attached. Initially, this approach conserved carbon atoms, required relatively few species, and both led to lower computational cost. However, as the mechanism evolved, its grouping increasingly resembled aggregated molecule schemes, since both molecular structure and total molecular weight significantly influence atmospheric chemistry (Yarwood et al., 2005). The disadvantage of CB mechanism is that chemical expression of free radicals is insufficient (Kang et al., 2016; Sarwar et al., 2008). Comparative analysis of different CB6 mechanism variants shows that differences in reaction pathways can lead to significant deviations in model predictions of ozone, NOx, and formaldehyde (Cao et al., 2021).
The Saprc series (Saprc -90, Saprc -99, Saprc -07) aggregate VOCs by molecule or functional group, representing roughly 400 categories. Condensed versions are widely used in urban and regional air quality models, but simplifications can limit the accuracy of organic chemistry representation (Stockwell et al., 2012). Comparative analyses of different Saprc variants reveal discrepancies in predicting ozone, radical species, and oxidative products, indicating

uncertainties arising from mechanism and emission inventories (Kang et al., 2025). For RACM, it was developed for broader applications, where NOx is lower and slower-reacting organics are more important. RACM version 2 includes 118 species and 356 reactions. Even though this mechanism is computationally efficient, however, it may inadequately capture detailed organic chemistry and secondary organic aerosol (SOA) formation, resulting with potential uncertainties in air quality predictions (Stockwell et al., 2012).

In air quality models, gas-phase chemical mechanisms are typically coupled with aerosol modules to simulate interactions between the gas and particulate phases. Aerosol Module 7 (aero7) is the latest aerosol representation within the CMAQ model (Byun and Schere, 2006), developed by the U.S. Environmental Protection Agency (EPA). Aero7 improves consistency in representing SOA formation pathways between the CB- and SAPRC-based chemical mechanisms. It also updates monoterpene SOA yields from photooxidation, adds uptake of water onto hydrophilic organics, and includes consumption of inorganic sulfates (SO_4^{2-}) when isoprene epoxydiol (IEPOX) organosulfates are formed (Pye et al., 2013). Furthermore, it enhances computational efficiency by using a volatility basis set (VBS) to parameterize SOA yields rather than using the Odum 2-product fit (Zhang et al., 2021a).

Most of the above chemical mechanisms and SOA treatment exhibit substantial limitations in simulating SOA formation (Wang et al., 2019; Zhang et al., 2021; Zhang et al., 2022; Zhang et al., 2023; Huang et al., 2024). First, Semi-Volatile Organic Compounds (SVOC) and Intermediate-Volatility Organic Compounds (IVOC) species are not explicitly represented, leading to an underestimation of SOA contribution from those precursors. Even in 2D-VBS mechanisms, which includes S/IVOC species, the gas-to-particle conversion of oxidative products are mainly characterized using empirical parameters (e.g., yields and volatility distributions). Moreover, the 2D-VBS framework does not explicitly track individual chemical reactions; instead, it relies on parameterizations derived from environmental chamber experiments or model calibration data, making it difficult to resolve specific chemical pathways of SOA formation (Chang et al., 2022). Second, the use of fixed-yield empirical parameterization limits the representation of multigenerational oxidative processes and gas-particle partitioning dynamics (Chang et al., 2022). Third, POA is commonly assumed to be non-volatile and non-reactive, thereby neglecting its potential for re-evaporation and subsequent oxidation to form SOA. These simplifications overly idealize SOA formation processes missing various key reactions and resulted in an inaccurate representation of the complex aging of organic aerosols in the atmosphere (Huang et al., 2024).

The Community Regional Atmospheric Chemistry Multiphase Mechanism (CRACMM) is the latest chemical mechanism developed under the leadership of scientists at the US EPA. CRACMM is built upon version 2 of RACM (Goliff et al., 2013) and incorporates state-of-the-science developments, including autoxidation, aromatic chemistry, oxygenated hydrocarbons, organic nitrates, and halogen chemistry. These advances enhance the representation of atmospheric chemical transformations, enabling more realistic simulations of key air pollutants such as O_3, $PM_{2.5}$, and various hazardous species, e.g. formaldehyde (Skipper et al., 2024). In addition, CRACMM integrates a full-volatility organic framework and explicitly accounts for multigenerational oxidative processes, thereby improving the physicochemical representation of secondary organic aerosol (SOA) formation and providing a more comprehensive description of SOA evolution (Ng et al., 2008).

CRACMM also provides detailed species mapping methodology between emission inventory and chemical mechanism(Pye et al., 2023), to ensure carbon conservation when tracking the transformation of carbon from emission sources to products (Ng et al., 2008). CB6r3_ae7 and Saprc07tic_ae7 do not consider certain SOA precursors such as L/S/IVOC (Chang et al., 2022), and CRACMM explicitly accounts for SOA precursors beyond traditional non-oxygenated volatile hydrocarbons, including phenolic compounds, furans, and other oxygenated organic species (Pye et al., 2023). This makes CRACMM describing and simulating SOA in more precise and accurate manner. No doubt CRACMM a good chemical mechanism candidate to address the above listed shortcomings. CRACMMv1.0 was applied in the simulation over northeast U.S. in summer reported in the work by Place et al (2023), and the result showed ozone simulated values were better than RACM2_ae6 chemical mechanism in terms of comparing with observation: average bias of RACM2_ae6 is +4.2ppb, average bias of CRACMMv1.0 +2.1 ppb. A few studies have been conducted using CRACMM but they all focused on US CONUS domain(Place et al., 2023). CRACMM has been not applied on China domain so thorough evaluation is a must.

(c)any computational cost related arguments

We made the following revisions accordingly.

Lines 151-158: For computational cost considerations, the number of species and reactions directly affects model runtime. Mechanisms with larger numbers of species and reactions, such as Saprc07tic_ae7i, which contains the largest number of reactions and species among the standard CMAQ mechanisms, is the most computational expensive mechanism compared to simpler mechanisms like CB6r3_ae7. In contrast, CB has fewer reactions and species. The primary difference between CB6r3_ae7 Saprc07tic_ae7i, and CRACMM lies in the chemistry module. Our tests indicate that CRACMM requires approximately 30 – 40% more computational time than CB6r3_ae7, but 20 – 30% less than Saprc.

(d) possible usage of complicated chemistry schemes in other regional scale models

We added the following text in the introduction section.

Lines 162-167: Also, CRACMM is not restricted to CMAQ. The design of CRACMM follows a modular framework for gas-phase chemistry and SOA formation, which does not rely on model-specific assumptions. Therefore, in principle, CRACMM could be implemented in other regional models, although additional effort would be required to adapt emission mapping and aerosol–chemistry coupling.

(e) potential to use an advanced chemical mechanism in global models (with an advancement in high performance computing).

We added related text in the introduction section.

Lines 159-162: With advances in high-performance computing, CRACMM could also be applied in a global scale. Particularly, the Model for Prediction Across Scales (MPAS) global meteorological model has recently been successfully coupled with CMAQ, demonstrating the application of CRACMM in the global MPAS-CMAQ coupled model framework (Wong et al.,

2024).

[1] Mao J, Li L, Li J, et al. Evaluation of Long-Term Modeling Fine Particulate Matter and Ozone in China During 2013–2019 [J]. 2022, Volume 10 - 2022.

[2] Emery C, Liu Z, Russell A G, et al. Recommendations on statistics and benchmarks to assess photochemical model performance [J]. Journal of the Air & Waste Management Association (1995), 2017, 67(5): 582-598.

[3] Meng F, Du X, Tang W, et al., Evaluation of Regional Atmospheric Models for Air Quality Simulations in the Winter Season in China. In *Atmosphere*, 2026; Vol. 17, p 1.

[4] Boylan J W Russell A G PM and light extinction model performance metrics, goals, and criteria for three-dimensional air quality models [J]. Atmospheric Environment, 2006, 40(26): 4946-4959.

[5] Yarwood G, Morris R E Wilson G M In *Particulate Matter Source Apportionment Technology (PSAT) in the CAMx Photochemical Grid Model*, Air Pollution Modeling and Its Application XVII, Boston, MA, 2007//, 2007; C Borrego; Norman A-L, Eds. Springer US: Boston, MA, 2007; pp 478-492.

[6] Kang M, Zhang H Ying Q Effectiveness of emission controls on atmospheric oxidation capacity and air pollutant concentrations: uncertainties due to chemical mechanisms and inventories [J]. Atmos. Chem. Phys., 2025, 25(18): 11453-11467.

[7] Yarwood G, Rao S, Yocke M, et al. Updates to the carbon bond chemical mechanism: CB05 final report to the US EPA [J]. RT-0400675, 2005.

[8] Inness A, Aben I, Ades M, et al. Assimilation of S5P/TROPOMI carbon monoxide data with the global CAMS near-real-time system [J]. Atmos. Chem. Phys., 2022, 22(21): 14355-14376.

[9] Wang Y, Ning M, Su Q, et al. Designing regional joint prevention and control schemes of PM2.5 based on source apportionment of chemical transport model: A case study of a heavy pollution episode [J]. Journal of Cleaner Production, 2024, 455: 142313.

[10] Yarwood G, Jung J, Whitten G Z, et al. In *UPDATES TO THE CARBON BOND MECHANISM FOR VERSION 6 (CB6)*, 2010; 2010.

[11] Kang Y-H, Oh I, Jeong J-H, et al. Comparison of CMAQ ozone simulations with two chemical mechanisms (SAPRC99 and CB05) in the Seoul metropolitan region [J]. 2016, 25(1): 85-97.

[12] Sarwar G, Luecken D, Yarwood G, et al. Impact of an updated carbon bond mechanism on predictions from the CMAQ modeling system: Preliminary assessment [J]. 2008, 47(1): 3-14.

[13] Cao L, Li S Sun L Study of different Carbon Bond 6 (CB6) mechanisms by using a concentration sensitivity analysis [J]. Atmos. Chem. Phys., 2021, 21(16): 12687-12714.

[14] Stockwell W R, Lawson C V, Saunders E, et al., A Review of Tropospheric Atmospheric Chemistry and Gas-Phase Chemical Mechanisms for Air Quality Modeling. In *Atmosphere*, 2012; Vol. 3, pp 1-32.

[15] Wang Y, Pavuluri C M, Fu P, et al. Characterization of Secondary Organic Aerosol Tracers over Tianjin, North China during Summer to Autumn [J]. ACS Earth and Space Chemistry, 2019, 3(10): 2339-2352.

[16] Zhang J, He X, Gao Y, et al. Assessing Regional Model Predictions of Wintertime SOA from Aromatic Compounds and Monoterpenes with Precursor-specific Tracers [J].

Aerosol and Air Quality Research, 2021, 21(12).
[17] Zhang J, He X, Ding X, et al. Modeling Secondary Organic Aerosol Tracers and Tracer-to-SOA Ratios for Monoterpenes and Sesquiterpenes Using a Chemical Transport Model [J]. Environmental Science & Technology, 2022, 56(2): 804-813.
[18] Zhang J, Liu J, Ding X, et al. New formation and fate of Isoprene SOA markers revealed by field data-constrained modeling [J]. npj Climate and Atmospheric Science, 2023, 6(1): 69.
[19] Huang L, Wu Z a, Liu H, et al. An improved framework for efficiently modeling organic aerosol (OA) considering primary OA evaporation and secondary OA formation from VOCs, IVOCs, and SVOCs [J]. Environmental Science: Atmospheres, 2024.
[20] Chang X, Zhao B, Zheng H, et al. Full-volatility emission framework corrects missing and underestimated secondary organic aerosol sources [J]. One Earth, 2022, 5(4): 403-412.
[21] Ng N L, Kwan A J, Surratt J D, et al. Secondary organic aerosol (SOA) formation from reaction of isoprene with nitrate radicals (NO_3) [J]. Atmospheric Chemistry and Physics, 2008, 8(14): 4117-4140.
[22] Goliff W S, Stockwell W R Lawson C V The regional atmospheric chemistry mechanism, version 2 [J]. Atmospheric Environment, 2013, 68: 174-185.
[23] Skipper T N, D'Ambro E L, Wiser F C, et al. Role of chemical production and depositional losses on formaldehyde in the Community Regional Atmospheric Chemistry Multiphase Mechanism (CRACMM) [J]. Atmospheric Chemistry and Physics, 2024, 24(22): 12903-12924.
[24] Pye H O T, Place B K, Murphy B N, et al. Linking gas, particulate, and toxic endpoints to air emissions in the Community Regional Atmospheric Chemistry Multiphase Mechanism (CRACMM) [J]. Atmospheric Chemistry and Physics, 2023, 23(9): 5043-5099.
[25] Place B K, Hutzell W T, Appel K W, et al. Sensitivity of northeastern US surface ozone predictions to the representation of atmospheric chemistry in the Community Regional Atmospheric Chemistry Multiphase Mechanism (CRACMMv1.0) [J]. Atmospheric Chemistry and Physics, 2023, 23(16): 9173-9190.

Minors:

L22: "…two traditional chemical mechanisms, CB6r3_ae7 and Saprc07tic_ae7i, for China." Kindly consider providing a longer name.

We thank the reviewer for this suggestion. We have revised the manuscript to provide the full names of the two traditional chemical mechanisms at their first occurrence in lines 22-24. We also clarified the evolution of Saprc07 to Saprc07tic.

The Saprc07t version differs from the standard Saprc07 mechanism (Carter, 2010) in that it includes additional explicit species, allowing a more accurate representation of reactive organic compounds (e.g., propene, ethanol, and 1,2,4-trimethylbenzene) and hazardous air pollutants such as acrolein, 1,3-butadiene, toluene, and xylene isomers. The Saprc07t mechanism implemented in CMAQ has two variants, Saprc07tb and Saprc07tc. These two variants include identical chemical species and yield the same predictions, differing only in the numerical

expressions of reaction rate constants(Hutzell et al., 2012). Saprc07tic represents an extended version of Saprc07t that incorporates a more detailed isoprene oxidation chemistry (Pye et al., 2013).

Lines 22-24: Carbon Bond 6 version r3 with aero7 treatment of SOA (CB6r3_ae7) and State Air Pollution Research Center version 07tc with extended isoprene chemistry and aero7i treatment of SOA (Saprc07tic_ae7i)

L25: "…show slight differences in the correlation coefficient…" Please provide a number.
We have revised the manuscript to quantify the term "slight" by explicitly stating that the differences in the correlation coefficient are smaller than 0.14 and 10μg/m^3 for mean bias (MB), and within 10% for normalized mean bias (NMB) values.

Lines 26-29: The results indicate that, when using the traditional primary organic aerosol (POA) inventory, the differences among the three chemical mechanisms are within 0 - 0.14 for the R, 0 - 10 μg/m^3 for the MB, and within 10% for the NMB values.

L28: Same comment as above.
Revised accordingly.

Lines 29-33: However, when the full-volatility emission inventory is applied in January, CRACMM exhibits improved performance in the PRD region. The MB is reduced by 3.0-7.8 μg/m^3. In addition, the NMB decreases by 17–23%, and the root mean square error (RMSE) is reduced by 1- 6 μg/m^3compared with simulations using the traditional POA inventory across the four months.

L41: Please consider citing a couple of more recent papers.
Thank you for the suggestion. We have added two more recent references.

Lines 44-45: Exposure to airborne $PM_{2.5}$ is associated with a variety of harmful health effects (Liu et al., 2024; Tsai et al., 2025; Kim et al., 2015)

Liu, J., Niu, X., Zhang, L., Yang, X., Zhao, P., and He, C.: Exposure risk assessment and synergistic control pathway construction for O_3 – $PM_{2.5}$ compound pollution in China, Atmos. Environ. X., 21, 100240,doi: 10.1016/j.aeaoa.2024.100240, 2024.
Tsai, Y. G., Wang, J. Y., Yang, K. D., Yang, H. Y., Yeh, Y. P., Chang, Y. J., Lee, J. H., Wang, S. L., Huang, S. K., and Chan, C. C.: Long-term PM(2.5) exposure impairs lung growth and increases airway inflammation in Taiwanese school children, ERJ open research, 11,doi: 10.1183/23120541.00972-2024, 2025.

L56: 'CMAQ' appears for the first time in the main text. Full name and citation needed.
Revised.
Lines 49-50: Chemical transport models such as Community Multiscale Air Quality (CMAQ) model (Byun and Schere, 2006) have been widely applied in China to investigate air quality

issues,

Byun, D. and Schere, K. L.: Review of the Governing Equations, Computational Algorithms, and Other Components of the Models-3 Community Multiscale Air Quality (CMAQ) Modeling System, Applied Mechanics Reviews, 59, 51-77,doi: 10.1115/1.2128636, 2006.

L114: Kindly add one of two citations to which the reader may refer to better understand the importance of these regions.

We have added two recent references to highlight the importance of the key regions discussed in our study in line 179. Specifically, we now cited two studies (Huang et al. (2024) and Deng et al. (2022)) to exemplify the significance of the five regions, BTH, YRD, PRD, FWP, and SCB, in terms of $PM_{2.5}$ pollution and air quality management.

Huang, L., Wu, Z. a., Liu, H., Yarwood, G., Huang, D., Wilson, G., Chen, H., Ji, D., Tao, J., Han, Z., Wang, Y., Wang, H., Huang, C., and Li, L.: An improved framework for efficiently modeling organic aerosol (OA) considering primary OA evaporation and secondary OA formation from VOCs, IVOCs, and SVOCs, Environmental Science: Atmospheres,doi: 10.1039/d4ea00060a, 2024.

Deng, C., Tian, S., Li, Z., and Li, K.: Spatiotemporal characteristics of $PM_{2.5}$ and ozone concentrations in Chinese urban clusters, Chemosphere, 295, 133813,doi: 10.1016/j.chemosphere.2022.133813, 2022.

L118: Kindly mention the physics and chemistry timesteps. I would also recommend adding a table in the supplement mentioning the different parameterizations used in the study.

We used the EBI chemistry solver in CMAQ evaluating all three chemical mechanisms for consistency. The chemistry time step in CMAQ is not a constant but it is automatically adjusted by the model based on the stiffness of the system of chemical reactions which are represented by an ordinary differential equations (ODEs) system, that CMAQ is solving. The physical transport processes such as advection and diffusion, are identical across all mechanisms. As a result, presenting physics and chemistry timestep in a table is not practical.

L128: Please consider removing the link and adding a citation for WRF.
Revised accordingly.

Lines 193-196: CMAQ ready meteorological input files were created by the Meteorology-Chemistry Interface Processor (MCIP) (Otte and Pleim, 2010) version 5.4 processing through output files from an offline run of the Weather Research and Forecasting (WRF) model version 4.0 (Skamarock et al., 2019).

Skamarock, W. C., Klemp., J., Dudhia., J., Gill., D. O., Liu., Z., and Berner., J.: A Description

of the Advanced Research WRF Model Version 4.1,doi: https://doi.org/10.5065/1dfh-6p97, 2019.

L135: Kindly mention the nominal resolution of the emissions and the sectors included.

The nominal resolution of the emissions used in this study is 0.25° × 0.25°. The emissions include five major sectors, including power, industry, residential, transportation, and agriculture. Please refer to page 8.

Lines 208-210: Its spatial resolution is 0.25° × 0.25° and includes five sectors: power, industry, residential, transportation, and agriculture,

L139: Consider removing the link or move it to the data availability section.

We have moved the MEGANv3.2 link from the main text to the Data Availability section, and revised the text accordingly.

Lines 774-776: Biogenic emissions were estimated using the MEGANv3.2 model (Guenther et al., 2012), which is available at https://bai.ess.uci.edu/megan/data-and-code/megan32.

Table S1: Kindly mention about E/L in the caption.

The figure caption has been updated as follows to clarify that "E" stands for explicit species and "L" stands for lumped species.

Table S5: The species mapping from Sarprc07tic_ae7i and CB6r3_ae7 to CRACMM used in CMAQ, where "E" stands for explicit species and "L" stands for lumped species.

Table S2: Consider adding the numbers for the different regions in China.
We have added regional aggregated values for different regions in China to Tables S1-S4. The regional totals are summarized based on the provincial emissions, and results for four representative months. The revised manuscript included the following statement in lines 210-211 and updated supplemental tables.

"and the provincial VOC emissions in 2019 from MEIC, categorized by sector for January, April, July, October are shown in Tables S1-S4.".

Table S1 Provincial VOC emissions in January 2019 from MEIC, categorized by sector. Unit: 10^3 tons /yr.

Regions	Power	Industry	Residential	Transportation	Agriculture
Beijing	0.01	2.54	0.62	0.69	0.00
Tianjin	0.01	2.47	0.34	0.39	0.00
Hebei	0.02	6.49	5.15	2.03	0.00
Shanxi	0.03	2.92	1.88	0.87	0.00
Inner Mongolia	0.05	3.03	2.55	0.74	0.00
Liaoning	0.02	5.35	2.33	1.02	0.00
Jilin	0.01	2.66	1.89	0.57	0.00
Heilongjiang	0.01	2.15	3.87	0.60	0.00
Shanghai	0.01	4.19	0.23	0.51	0.00
Jiangsu	0.06	11.95	2.71	2.50	0.00
Zhejiang	0.03	10.25	1.32	2.07	0.00
Anhui	0.02	4.20	3.76	1.16	0.00
Fujian	0.01	5.95	1.17	0.95	0.00
Jiangxi	0.01	3.35	1.28	0.76	0.00
Shandong	0.05	11.07	4.04	2.99	0.00
Henan	0.03	5.17	2.30	1.96	0.00
Hubei	0.01	5.06	5.34	1.08	0.00
Hunan	0.01	4.08	5.94	1.03	0.00
Guangdong	0.04	10.86	1.70	3.07	0.00
Guangxi	0.01	5.65	1.36	0.92	0.00
Hainan	0.00	0.83	0.25	0.20	0.00
Chongqing	0.01	2.46	2.05	0.55	0.00
Sichuan	0.00	5.86	5.71	1.51	0.00
Guizhou	0.02	1.50	7.48	0.61	0.00
Yunnan	0.00	3.34	2.47	1.09	0.00
Tibet	0.00	0.01	0.41	0.06	0.00
Shaanxi	0.02	2.91	2.07	0.84	0.00
Gansu	0.01	1.09	1.31	0.45	0.00
Qinghai	0.00	0.36	0.21	0.15	0.00
Ningxia	0.01	0.70	0.24	0.20	0.00
Xinjiang	0.03	2.21	1.79	0.59	0.00
Total	0.55	130.62	73.79	32.14	0.00

Table S2 Provincial VOC emissions in April 2019 from MEIC, categorized by sector. Unit: 10^3 tons /yr.

Regions	Power	Industry	Residential	Transportation	Agriculture
Beijing	0.01	2.25	0.27	0.70	0.00
Tianjin	0.01	2.86	0.12	0.41	0.00
Hebei	0.02	7.85	1.57	2.07	0.00
Shanxi	0.03	3.27	0.45	0.89	0.00
Inner Mongolia	0.04	3.57	1.02	0.74	0.00
Liaoning	0.01	6.08	1.03	1.05	0.00
Jilin	0.01	2.63	0.79	0.58	0.00
Heilongjiang	0.01	2.74	1.53	0.60	0.00
Shanghai	0.01	4.22	0.22	0.53	0.00
Jiangsu	0.05	12.04	1.45	2.62	0.00
Zhejiang	0.03	11.63	0.90	2.18	0.00
Anhui	0.02	4.32	1.14	1.21	0.00
Fujian	0.01	6.04	1.14	0.98	0.00
Jiangxi	0.01	3.92	0.75	0.80	0.00
Shandong	0.04	15.03	1.71	3.06	0.00
Henan	0.02	6.62	0.84	2.05	0.00
Hubei	0.01	6.12	1.54	1.13	0.00
Hunan	0.00	4.44	1.67	1.08	0.00
Guangdong	0.04	11.42	1.67	3.14	0.00
Guangxi	0.00	3.14	1.32	0.94	0.00
Hainan	0.00	0.70	0.25	0.20	0.00
Chongqing	0.00	2.97	0.61	0.57	0.00
Sichuan	0.00	6.59	1.60	1.55	0.00
Guizhou	0.02	1.53	1.89	0.64	0.00
Yunnan	0.00	3.15	1.28	1.11	0.00
Tibet	0.00	0.07	0.16	0.06	0.00
Shaanxi	0.01	3.39	0.64	0.86	0.00
Gansu	0.01	1.34	0.30	0.46	0.00
Qinghai	0.00	0.49	0.09	0.15	0.00
Ningxia	0.01	0.85	0.11	0.20	0.00
Xinjiang	0.02	2.76	0.72	0.60	0.00
Total	0.44	144.05	28.74	33.18	0.00

Table S3 Provincial VOC emissions in July 2019 from MEIC, categorized by sector. Unit: 10^3 tons /yr.

Regions	Power	Industry	Residential	Transportation	Agriculture
Beijing	0.01	2.32	0.27	0.70	0.00
Tianjin	0.01	2.68	0.12	0.41	0.00
Hebei	0.02	7.87	1.59	2.12	0.00
Shanxi	0.03	3.65	0.46	0.92	0.00
Inner Mongolia	0.05	3.56	0.59	0.78	0.00
Liaoning	0.02	6.46	0.67	1.07	0.00
Jilin	0.01	2.85	0.49	0.60	0.00
Heilongjiang	0.01	2.82	0.88	0.63	0.00
Shanghai	0.01	4.01	0.22	0.55	0.00
Jiangsu	0.06	11.74	1.46	2.62	0.00
Zhejiang	0.02	11.57	0.91	2.32	0.00
Anhui	0.02	4.41	1.17	1.27	0.00
Fujian	0.01	5.77	1.17	1.03	0.00
Jiangxi	0.01	4.00	0.77	0.84	0.00
Shandong	0.04	14.59	1.73	3.13	0.00
Henan	0.03	7.18	0.86	2.05	0.00
Hubei	0.01	5.97	1.58	1.13	0.00
Hunan	0.01	4.57	1.72	1.15	0.00
Guangdong	0.05	11.74	1.70	3.33	0.00
Guangxi	0.00	3.22	1.36	0.99	0.00
Hainan	0.00	0.59	0.25	0.21	0.00
Chongqing	0.00	2.73	0.62	0.57	0.00
Sichuan	0.00	6.66	1.64	1.59	0.00
Guizhou	0.01	1.61	1.95	0.64	0.00
Yunnan	0.00	2.76	1.32	1.11	0.00
Tibet	0.00	0.08	0.08	0.07	0.00
Shaanxi	0.01	3.38	0.65	0.88	0.00
Gansu	0.00	1.35	0.31	0.47	0.00
Qinghai	0.00	0.47	0.06	0.15	0.00
Ningxia	0.01	0.96	0.07	0.21	0.00
Xinjiang	0.03	2.95	0.42	0.61	0.00
Total	0.52	144.52	27.09	34.14	0.00

Table S4 Provincial VOC emissions in October 2019 from MEIC, categorized by sector. Unit: 10^3 tons /yr.

Regions	Power	Industry	Residential	Transportation	Agriculture
Beijing	0.01	2.47	0.27	0.69	0.00
Tianjin	0.01	3.04	0.12	0.40	0.00
Hebei	0.02	8.26	1.59	2.07	0.00
Shanxi	0.03	3.34	0.46	0.89	0.00
Inner Mongolia	0.05	4.36	1.05	0.74	0.00
Liaoning	0.01	5.67	1.05	1.05	0.00
Jilin	0.01	2.93	0.81	0.57	0.00
Heilongjiang	0.01	3.12	1.57	0.60	0.00
Shanghai	0.01	4.64	0.22	0.53	0.00
Jiangsu	0.05	11.59	1.46	2.62	0.00
Zhejiang	0.02	12.46	0.91	2.18	0.00
Anhui	0.02	5.13	1.17	1.21	0.00
Fujian	0.01	6.68	1.17	0.98	0.00
Jiangxi	0.01	4.67	0.77	0.80	0.00
Shandong	0.04	14.22	1.73	3.13	0.00
Henan	0.02	7.51	0.86	2.05	0.00
Hubei	0.01	5.44	1.58	1.13	0.00
Hunan	0.01	5.38	1.72	1.08	0.00
Guangdong	0.04	13.84	1.70	3.14	0.00
Guangxi	0.01	3.55	1.36	0.94	0.00
Hainan	0.00	0.81	0.25	0.20	0.00
Chongqing	0.00	3.01	0.62	0.57	0.00
Sichuan	0.00	7.29	1.64	1.55	0.00
Guizhou	0.02	1.83	1.95	0.64	0.00
Yunnan	0.00	3.12	1.32	1.11	0.00
Tibet	0.00	0.05	0.16	0.06	0.00
Shaanxi	0.01	4.19	0.65	0.86	0.00
Gansu	0.01	1.57	0.31	0.46	0.00
Qinghai	0.00	0.49	0.10	0.15	0.00
Ningxia	0.01	1.11	0.07	0.20	0.00
Xinjiang	0.03	3.75	0.74	0.60	0.00
Total	0.45	155.52	29.37	33.21	0.00

All the lat-lon figures seem crowded. Kindly consider removing some of the background colors.

We believe the reviewer is referring to Figure 1 only. We have revised Fig. 1 by reducing the number of latitude–longitude grid lines and updating the background colors, to improve the overall readability of the figure.

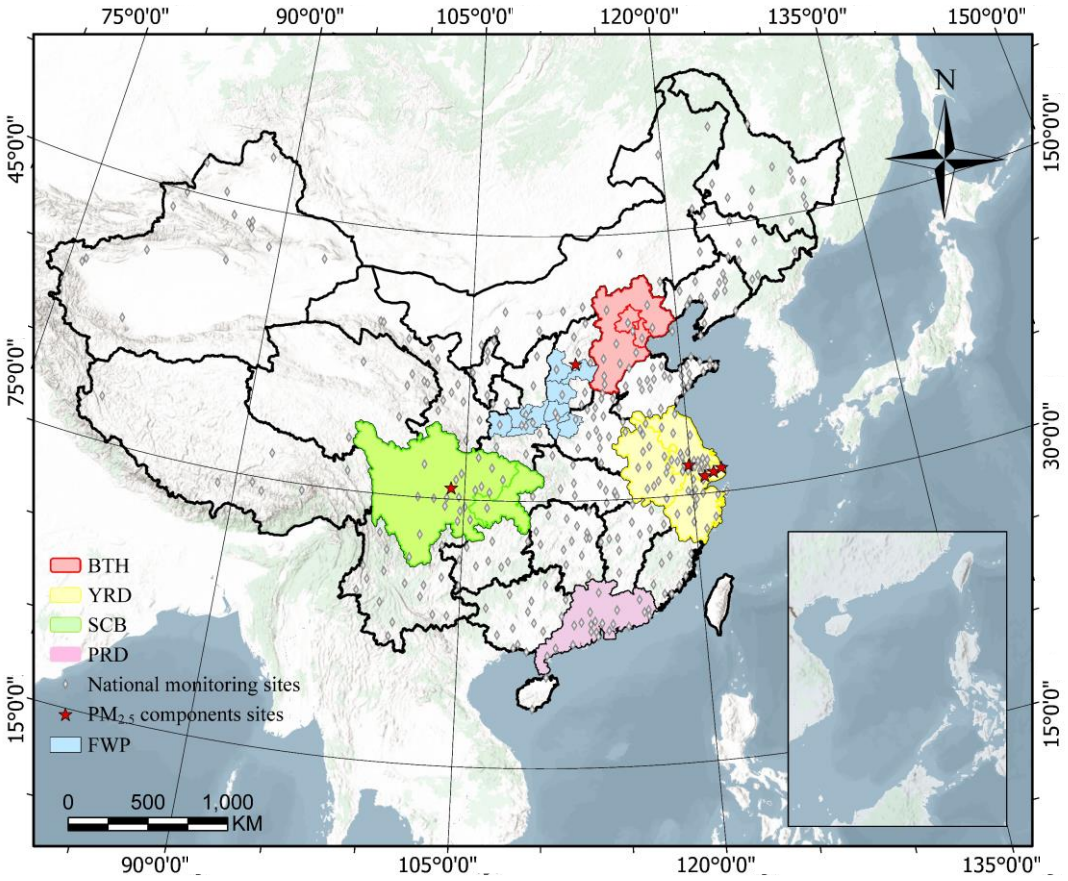

L226: I recommend adding a couple of maps showing monthly average precipitation and monthly average PBL (or histograms if the authors prefer that).

We have added plots of monthly total precipitation (Fig. S5), and monthly mean PBL height (Fig. S6). These two additional diagnostics help illustrating the meteorological conditions and their potential influence on air pollutant concentrations during the study period. The manuscript has been revised accordingly.

Lines 334-338: This decline is mainly attributable to the increased precipitation which washed out pollutants, in the southern and eastern parts of China compared to other months (Figure S5) In addition, higher planetary boundary layer (PBL) heights during the warm season in the south, particularly in the YRD region of China than other months (Figure S6), enhancing atmospheric mixing and dilution, and led to the decrease in $PM_{2.5}$ concentrations.

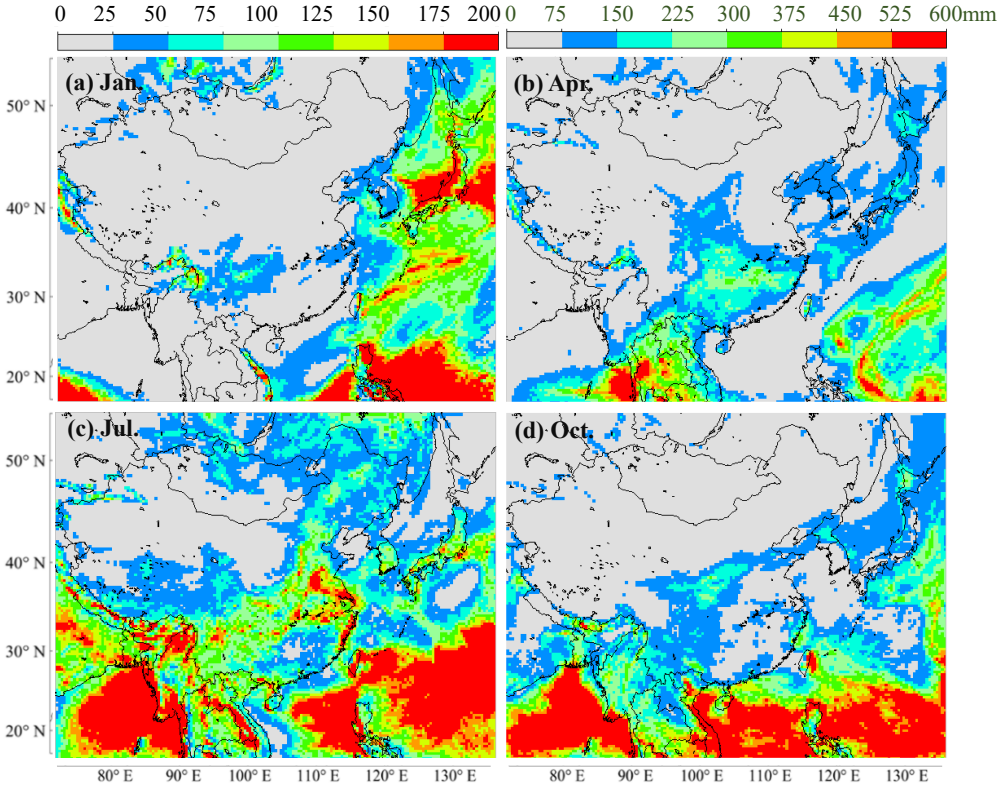

Figure S5 Spatial distribution of monthly total precipitation (mm). Note: Panels (a), (b), and (d) share a common color bar (top left), whereas panel (c) uses a separate color bar (top right) to better highlight spatial variations

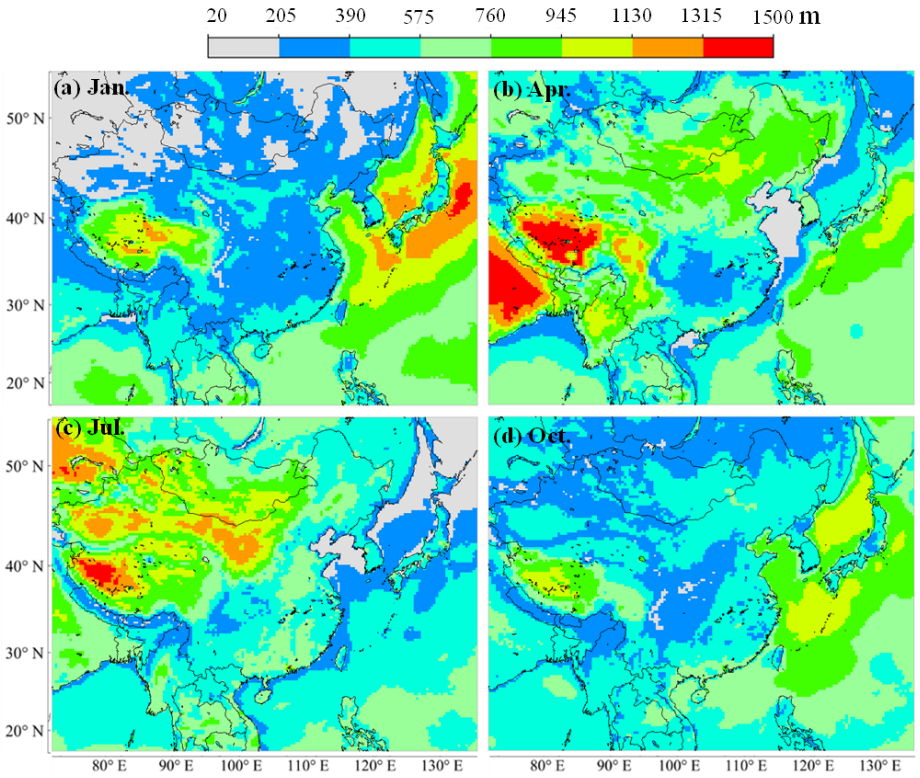

Figure S6 Spatial distribution of monthly mean PBL height (m).

Figure 2: The choice of color scale is such that extreme low PM2.5 (0-5 µg/m^3) is coinciding with the white background and making it difficult to interpret the figures. Please fix the colorscale.

We have adjusted the color scale in the figures so that low $PM_{2.5}$ values (0–5 µg/m³) are now more distinguishable from the white background, improving the readability of the figures. The revised figures are shown below.

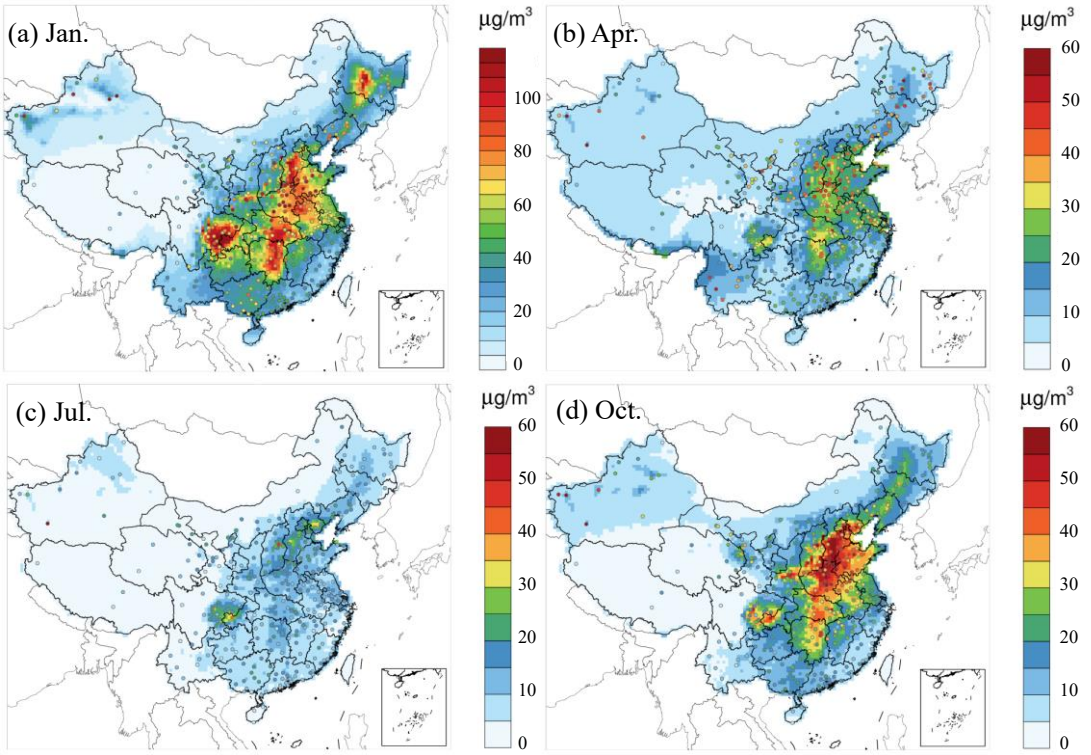

L236-L248: The current description could be improved. The correlation co-efficient is one statistical metric. I would encourage the authors to shorten this description and focus on the scientific understanding. Additionally consider adding a couple of sentences in the supplement describing how dust concentrations are calculated in the model (an empirical function of wind speed?)

We have revised the description as follows. First, the text in lines 236–248 has been shortened and revised to focus on the physical interpretation of the results. Second, in the current study, CMAQ was not configured with dust emissions, so dust module was not turned on. We acknowledge the importance of dust in contribution of $PM_{2.5}$ and will consider turning on dust model in the future study.

Lines 349-357: In January, CRACMM shows higher R value (R>0.7) over northern China (e.g.,

BTH, FWP), whereas lower R values (approximately 0.4) are found in southern regions (e.g., PRD) (Figure 3a). The model generally underestimates $PM_{2.5}$ across most areas (Figure 4a), except for the YRD and SCB regions, where positive biases occur at many sites. This spatial contrast is partly attributable to dust-related influences, although data from the major dust episode on 13-14 January were excluded from the monthly evaluation, the absence of explicit dust emissions and the associated complex meteorological conditions likely contributed to $PM_{2.5}$ underestimation of up to ~30 μg/m^3 in northern China.

In the supplement, please add an equation for R and NMB. I also encourage the authors to report Normalized Root Mean Squared Error.

We have added equations for R and NMB in Table S10 and added descriptions. In addition, we have calculated and reported RMSE as another statistical metric in model performance evaluation in Figure S12.

Lines 317-323: The formulas for each individual parameter are presented in Table S10. In these equations, $\bar{C_m}$ and $\bar{C_o}$ represent the mean modeled and observed concentrations over all samples, respectively; C_m and C_o denote the modeled and observed values for the i-th sample; and N is the total number of valid samples. A combined analysis of these statistical indicators enables a comprehensive assessment of model performance and reliability, providing a basis for further model refinement and interpretation of the simulation results.

Table S10 Definition of model performance evaluation metrics used in this study

Statistical metrics	Definition	Units
MB	$MB = \frac{1}{N}\sum_{i=1}^{N}(C_m - C_o)$	μg/m^3
NMB	$NMB = \frac{\sum_{i=1}^{N}(C_m - C_o)}{\sum_{i=1}^{N} C_o} \times 100\%$	%
NME	$NME = \frac{\sum_{i=1}^{N}\lvert C_m - C_o\rvert}{\sum_{i=1}^{N} C_o} \times 100\%$	%
RMSE	$RMSE = \sqrt{\frac{1}{N}\sum_{i=1}^{N}(C_m - C_0)^2}$	μg/m^3
R	$R = \frac{\sum_{i=1}^{N}(C_m - \overline{C_m})(C_o - \overline{C_o})}{\sqrt{\sum_{i=1}^{N}(C_m - \overline{C_m})}\sqrt{\sum_{i=1}^{N}(C_o - \overline{C_o})}}$	/

IOA	$IOA = 1 - \frac{\sum_{i=1}^{N}(C_m - C_o)^2}{\sum_{i=1}^{N}(\lvert C_m - \overline{C_0}\rvert + \lvert C_0 - \overline{C_0}\rvert)^2}$	/

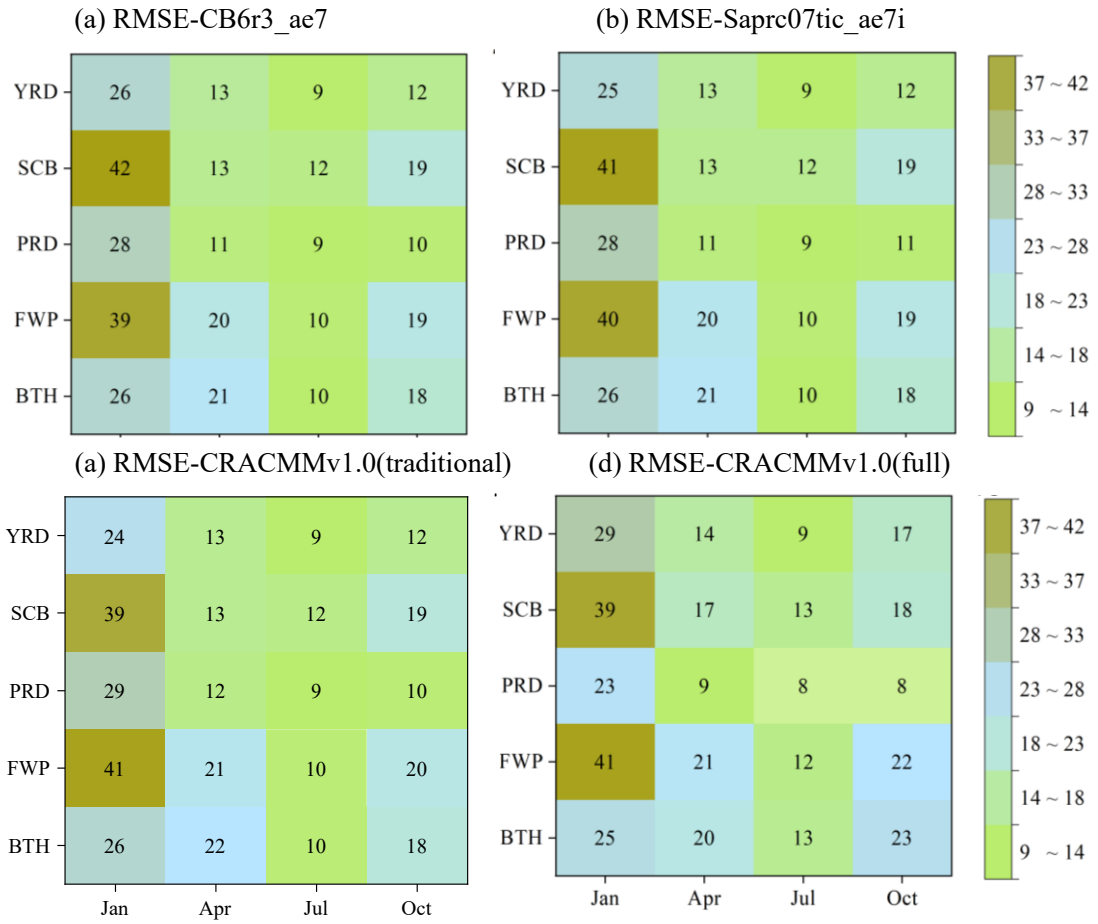

Figure S12. RMSE (μg/m^3) across five regions (YRD, SCB, PRD, FWP, BTH) and four months (January, April, July, and October) for (a) CB6r3_ae7, (b) Saprc07tic_ae7i, (c) CRACMM with traditional POA inventory, and (d) CRACMM with full volatile POA inventory.

L286-287: I recommend adding evidence for this conclusion.

Springtime dust events, which reduce photolysis rates, frequently occur in northern China (Huo et al., 2025). In contrast, photochemical activity generally peaks in summer (June-August) due to strong solar radiation and high temperatures (Gu et al., 2022). Lower R for wind speed and temperature are observed in July, indicating uncertainty in meteorology which can lead to chemical variability. Therefore, the discrepancies observed in April and July can be reasonably attributed to these combined meteorological and photochemical factors. We have revised the text accordingly.

Lines 393-402: However, discrepancies arise in April, likely due to chemical conditions such as dust storms, springtime dust events are frequently observed in China, particularly in northern regions, driven by strong surface winds and synoptic-scale transport (Huo et al., 2025). For July, larger discrepancies are likely associated with more complex meteorological conditions, as reflected by the relatively poor performance of wind speed, particularly in the SCB region. In contrast, the simulation performance of relative humidity and temperature shows only minor differences relative to the other three months (Tables S11–S13).In addition, photochemical activity typically peaks in the summer months (June-August) due to stronger solar radiation and higher temperatures (Gu et al., 2022), which further exacerbates these discrepancies.

L299: Fix the sentence.

Revised.

Lines 414-415: Tables S14-S17 summarize the statistical values of $PM_{2.5}$ components, including NO_3^-, SO_4^{2-}, NH_4^+, OC, and EC, for the four selected months.

Table 2: It is not clear how the recommended benchmark is calculated. It seems that the correlation is lower than the 'recommendation'. I would encourage the authors to add additional relevant literature and discussion.

The recommended benchmarks are derived from previous studies(Huang et al., 2021) and directly cited in this work. They are literature-based analysis of $PM_{2.5}$ modeling studies, where rank-ordered distributions of performance metrics are used to define the 33rd and 67th percentile thresholds following Simon et al. (2012) and Emery et al. (2017). In the revised manuscript, we discuss the comparison of model performance evaluation results between this study and those of other studies.

The R is lower than the 'recommendation', it can be attributed to the uncertainty of MEIC and S/IVOC emissions inventory and meteorological information is an essential input to each air quality simulation (along with emissions, boundary concentrations, etc.) and uncertainties in the meteorology will inevitably influence the air quality simulation to some degree(Huang et al., 2021).

Although the R is lower than the recommended value, according to previous study, the R of the five regions across different months is also below 0.6. Meteorology is an essential component

of air quality simulations, together with emissions and boundary conditions, and uncertainties in meteorological fields inevitably propagate into the simulated air pollutant concentrations (Huang et al., 2021). Uncertainties in the MEIC and S/IVOC emission inventory is another potential cause of the lower R value.

Lines 431-438: Previous studies have reported similar R values. For example, the evaluation results of $PM_{2.5}$ simulations using CMAQ over five key regions in China，which is consistent with the regions considered in this study，showed that the R were generally below 0.6 in July (Huang et al., 2024). In addition, a multi-model intercomparison study involving CAMx6.2, CAMx7.1, CMAQv5.0.2 and CMAQv5.3.2 reported R values of 0.58, 0.55, 0.60, and 0.39, respectively, for mean $PM_{2.5}$ concentrations in China during 2014–2017. The CAMx6.2, CAMx7.1, and CMAQv5.0.2 simulations covered the entire country, whereas CMAQv5.3.2 was evaluated over eastern China (Meng et al., 2026).

L331: Evidence needed.

Traditional POA inventory does not include key precursors such as S/IVOCs, and this has been explained in line 290-291. “The new inventory fills a gap of 3,610 kt/y in L/S/IVOC emissions that were absent from the traditional inventory”

Some of the 4 panel figures have different color scales for different subplots. Please fix the colorscale or mention about different ranges in the caption.

The color scales have been harmonized across subplots where feasible. For subplots with substantially different data ranges, the varying color scales are retained to preserve detail, and the differences are explicitly described in the figure captions for Figures 2, 7, S5, S17, S19.

Section 3.3.2: A brief description of the C_i^* and its importance could be beneficial for the readers.

We have added a brief description of the effective saturation concentration ($Ci*$) and its importance in controlling organic aerosol volatility and gas–particle partitioning. This addition helps clarify why differences in $Ci*$ treatment between CRACMM and CB6r3_ae7 can lead to discrepancies in simulated POA concentrations. Revised text can be found in lines 568-569.

C_i^* represents the effective saturation concentration, which characterizes the volatility of organic compounds and influences gas-particle partitioning.

L462: Chang et al. – Fix.

Revised.

Chang et al. (2022)

L443: A longer description of the species' is recommended.

We have added a longer and clearer description of the species in the revised manuscript in lines 572-576 and 577-580.

where the numbers indicate negative (N) or positive (P) $log_{10}(C_i^*[\mu g/m^3])$ value. When species reside in the gas-phase as a vapor, it is prefixed with a "V" and when in the particle phase, a prefix "A" is used. For example, VROCP2ALK is an alkane-like vapor species with C_i^* of 10^2 μg/m^3, and AROCP2ALK is a particulate species of the same volatility.

these species follow a similar naming convention as the L/S/IVOC alkanes, where numbers after N and P indicate negative or positive $log_{10}(C_i^*)$ value and the value ends in $10\times nO{:}nC$ (e.g., ROCN2OXY2 is $C_i^* = 10^{-2}$ μg/m^3 with $nO{:}nC$ =0.2).

I would recommend the authors to add a simple flowchart to demonstrate different species in different mechanisms and their sources and sinks.

Following this recommendation, we have added simple schematic flowcharts illustrating the major species represented in different chemical mechanisms and their primary sources and sinks. The flowcharts focus on key species relevant to gas-phase chemistry and aerosol formation, and are intended to provide a clear conceptual comparison, rather than an exhaustive reaction-level description. The new figures have been added to the Supplementary Material as Figure S2 (CRACMM) and Figure S3 (CB6r3_ae7) accompanied with additional text to describe those figures. For the Saprc mechanism, the species representation and chemical pathways have already been described in detail a previous studies (Pye et al., 2015) and it is shown below but not included in this manuscript to avoid redundancy. A couple sentences were added in the manuscript reflecting this.

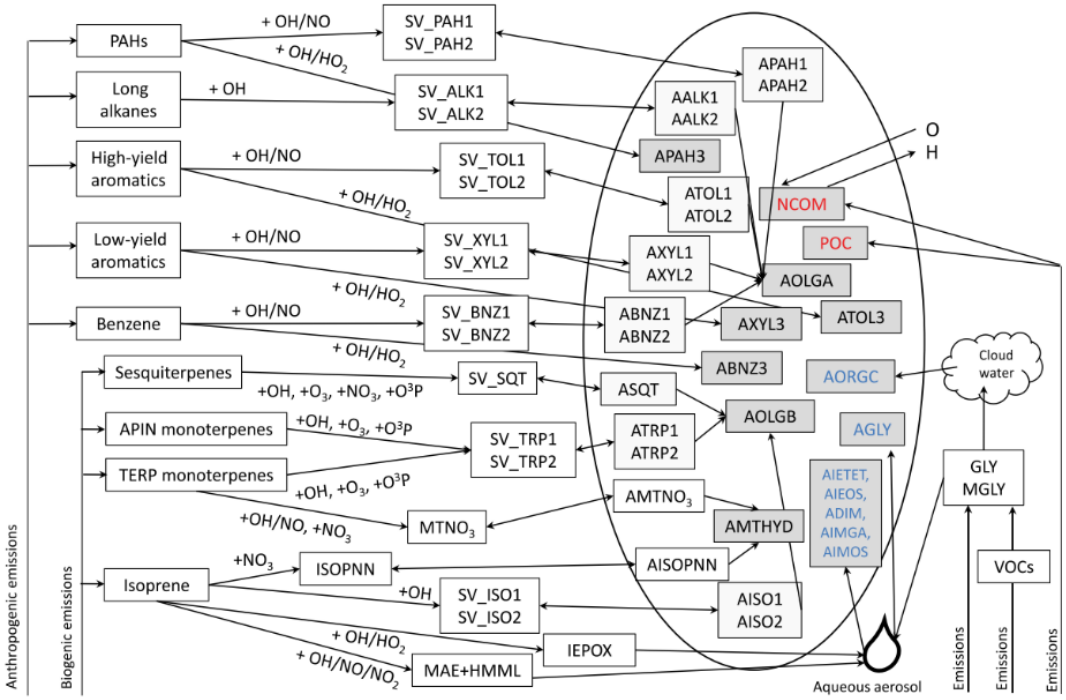

Schematic of SOA treatment in current CMAQ-aero6i (Pye et al., 2015).

Lines 188-190: Simple flowcharts illustrating the different species represented in each mechanism and their sources and sinks are shown in Figure S2 for CRACMM and Figure S3 for CB6r3_ae7. For Saprc07tic_ae7i,it has been described in detail in a previous studies(Pye et al., 2015).

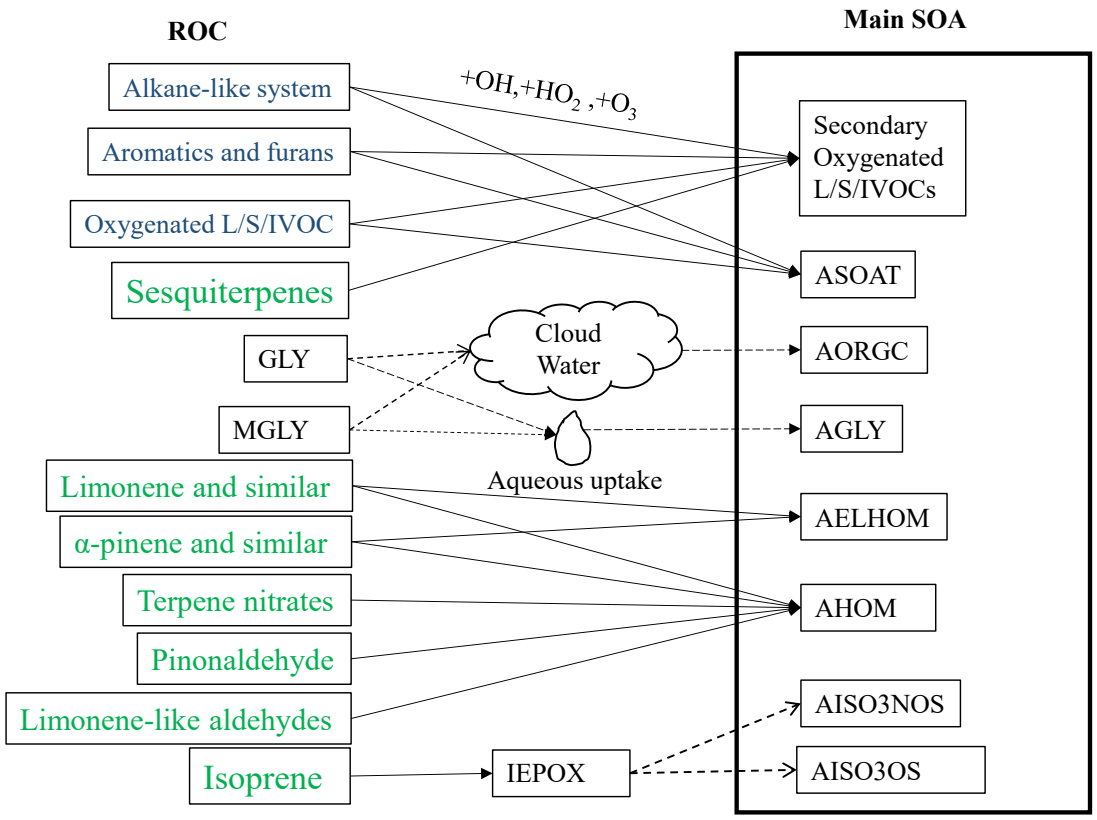

Figure S2. Treatment of SOA chemistry within the CRACMM mechanism in the CMAQv5.4 model. The thick black box surrounds all aerosol-phase species. Single-headed arrows represent irreversible processes. Dashed lines represent processes that modulated by the abundance of liquid water in the condensed phase. Species in dark blue are treated as anthropogenic species, and in green are treated as Biogenic species. The definitions of all surrogates are provided in Pye et al. (2023).

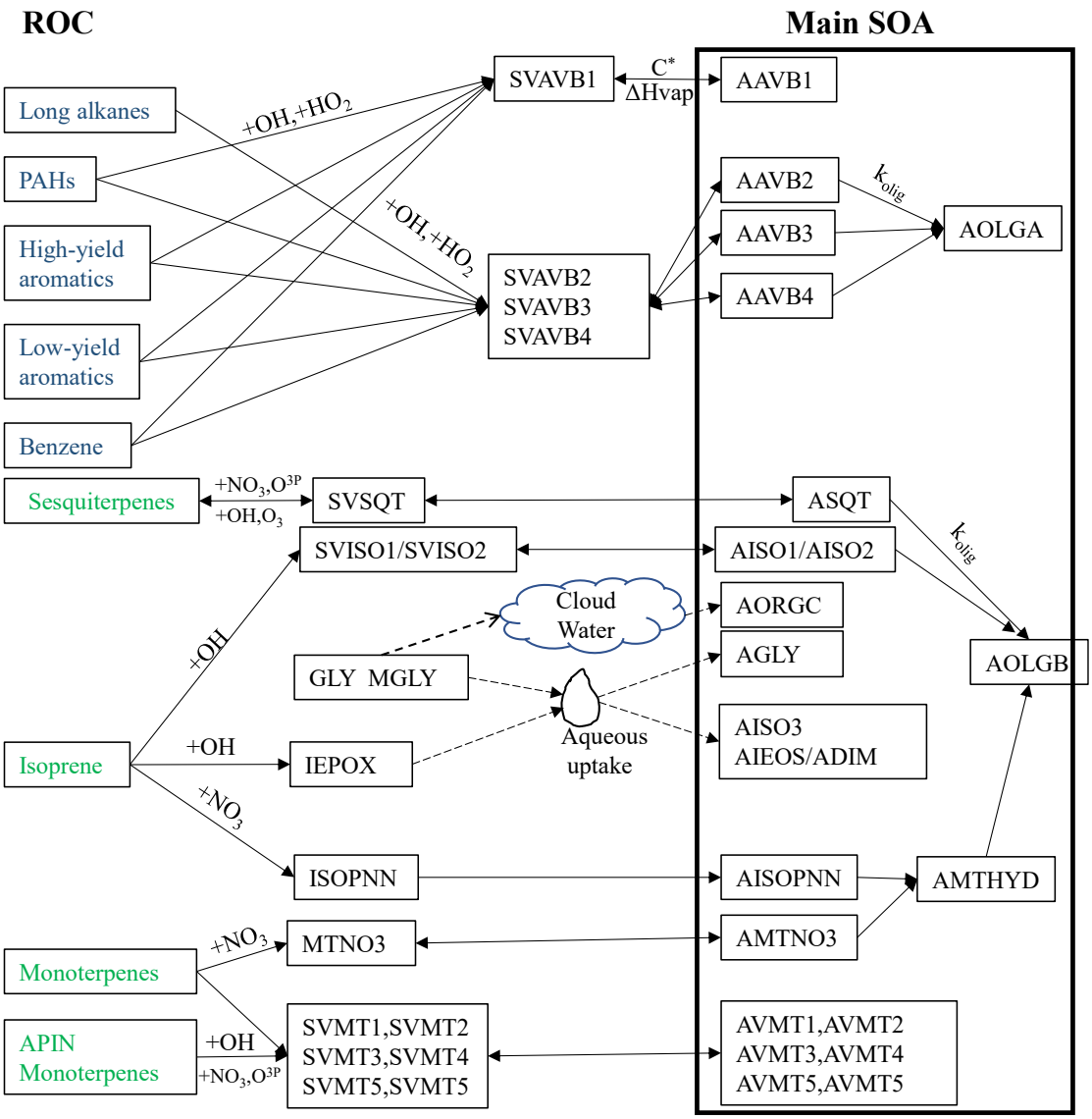

Figure S3. Treatment of SOA chemistry within the CB6 mechanism, including the mapping between chemical precursors and model species, in the CMAQv5.4 model in AERO7 (https://www.epa.gov/cmaq/how-cite-cmaq). The thick black box surrounds all aerosol-phase species. Double-headed arrows represent reversible processes, and single-headed arrows represent irreversible processes. Dashed lines represent processes that are dependent on the abundance of liquid water in the condensed phase. Species in dark blue are treated as anthropogenic species, and green are treated as biogenic species.

Note：Some other revisions have also been made. Please refer to the tracked-changes files for details. The newly added figures and the updated data have also been uploaded to a new version on Zenodo, and the manuscript has been revised accordingly.

Boylan, J. W. and Russell, A. G.: PM and light extinction model performance metrics, goals, and criteria for three-dimensional air quality models, Atmospheric Environment, 40, 4946-4959,doi: https://doi.org/10.1016/j.atmosenv.2005.09.087, 2006.

Byun, D. and Schere, K. L.: Review of the Governing Equations, Computational Algorithms, and Other Components of the Models-3 Community Multiscale Air Quality (CMAQ) Modeling System, Applied Mechanics Reviews, 59, 51-77,doi: 10.1115/1.2128636, 2006.

Cao, L., Li, S., and Sun, L.: Study of different Carbon Bond 6 (CB6) mechanisms by using a concentration sensitivity analysis, Atmos. Chem. Phys., 21, 12687-12714,doi: 10.5194/acp-21-12687-2021, 2021.

Carter, W. P. L.: Development of the SAPRC-07 chemical mechanism, Atmospheric Environment, 44, 5324-5335,doi: https://doi.org/10.1016/j.atmosenv.2010.01.026, 2010.

Chang, X., Zhao, B., Zheng, H., Wang, S., Cai, S., Guo, F., Gui, P., Huang, G., Wu, D., Han, L., Xing, J., Man, H., Hu, R., Liang, C., Xu, Q., Qiu, X., Ding, D., Liu, K., Han, R., Robinson, A. L., and Donahue, N. M.: Full-volatility emission framework corrects missing and underestimated secondary organic aerosol sources, One Earth, 5, 403-412,doi: 10.1016/j.oneear.2022.03.015, 2022.

Emery, C., Liu, Z., Russell, A. G., Odman, M. T., Yarwood, G., and Kumar, N.: Recommendations on statistics and benchmarks to assess photochemical model performance, Journal of the Air & Waste Management Association (1995), 67, 582-598,doi: 10.1080/10962247.2016.1265027, 2017.

Goliff, W. S., Stockwell, W. R., and Lawson, C. V.: The regional atmospheric chemistry mechanism, version 2, Atmospheric Environment, 68, 174-185,doi: https://doi.org/10.1016/j.atmosenv.2012.11.038, 2013.

Gu, J., Chen, Z., Zhang, N., Peng, S., Cui, W., Huo, G., and Chen, F.: Characterization of Atmospheric Fine Particles and Secondary Aerosol Estimated under the Different Photochemical Activities in Summertime Tianjin, China, International journal of environmental research and public health, 19,doi: 10.3390/ijerph19137956, 2022.

Guenther, A. B., Jiang, X., Heald, C. L., Sakulyanontvittaya, T., Duhl, T., Emmons, L. K., and Wang, X.: The Model of Emissions of Gases and Aerosols from Nature version 2.1 (MEGAN2.1): an extended and updated framework for modeling biogenic emissions, Geoscientific Model Development, 5, 1471-1492,doi: 10.5194/gmd-5-1471-2012, 2012.

Harrison, R. M., Beddows, D. C. S., Tong, C., and Damayanti, S.: Non-linearity of secondary pollutant formation estimated from emissions data and measured precursor-secondary pollutant relationships, npj Climate and Atmospheric Science, 5, 71,doi: 10.1038/s41612-022-00297-9, 2022.

Huang, L., Zhu, Y., Zhai, H., Xue, S., Zhu, T., Shao, Y., Liu, Z., Emery, C., Yarwood, G., Wang, Y., Fu, J., Zhang, K., and Li, L.: Recommendations on benchmarks for numerical air quality model applications in China – Part 1: PM2.5 and chemical species, Atmospheric Chemistry and Physics, 21, 2725-2743,doi: 10.5194/acp-21-2725-2021, 2021.

Huang, L., Wu, Z. a., Liu, H., Yarwood, G., Huang, D., Wilson, G., Chen, H., Ji, D., Tao, J., Han, Z., Wang, Y., Wang, H., Huang, C., and Li, L.: An improved framework for efficiently modeling organic aerosol (OA) considering primary OA evaporation and secondary OA formation from VOCs, IVOCs, and SVOCs, Environmental Science: Atmospheres,doi: 10.1039/d4ea00060a, 2024.

Huo, Q., Yin, Z., Ma, X., and Wang, H.: Distinctive dust weather intensities in North China resulted from two types of atmospheric circulation anomalies, Atmos. Chem. Phys., 25, 1711-1724,doi: 10.5194/acp-25-1711-2025, 2025.

Hutzell, W. T., Luecken, D. J., Appel, K. W., and Carter, W. P. L.: Interpreting predictions from the SAPRC07 mechanism based on regional and continental simulations, Atmospheric Environment, 46, 417-429,doi: https://doi.org/10.1016/j.atmosenv.2011.09.030, 2012.

Kang, M., Zhang, H., and Ying, Q.: Effectiveness of emission controls on atmospheric oxidation capacity and air pollutant concentrations: uncertainties due to chemical mechanisms and inventories, Atmos. Chem. Phys., 25, 11453-11467,doi: 10.5194/acp-25-11453-2025, 2025.

Kang, Y.-H., Oh, I., Jeong, J.-H., Bang, J.-H., Kim, Y.-K., Kim, S., Kim, E., Hong, J.-H., and Lee, D.-G. J. J. o. E. S. I.: Comparison of CMAQ ozone simulations with two chemical mechanisms (SAPRC99 and CB05) in the Seoul metropolitan region, 25, 85-97, 2016.

Kim, K.-H., Kabir, E., and Kabir, S.: A review on the human health impact of airborne particulate matter, Environment International, 74, 136-143,doi: https://doi.org/10.1016/j.envint.2014.10.005, 2015.

Liu, J., Niu, X., Zhang, L., Yang, X., Zhao, P., and He, C.: Exposure risk assessment and synergistic control pathway construction for O3–PM2.5 compound pollution in China, Atmospheric Environment: X, 21, 100240,doi: https://doi.org/10.1016/j.aeaoa.2024.100240, 2024.

Mao, J., Li, L., Li, J., Sulaymon, I. D., Xiong, K., Wang, K., Zhu, J., Chen, G., Ye, F., Zhang, N., Qin, Y., Qin, M., and Hu, J.: Evaluation of Long-Term Modeling Fine Particulate Matter and Ozone in China During 2013–2019, Volume 10 - 2022,doi: 10.3389/fenvs.2022.872249, 2022.

Meng, F., Du, X., Tang, W., He, J., Li, Y., Wang, X., Yu, S., Tang, X., Xing, J., Xie, M., Zeng, L., and Dong, H.: Evaluation of Regional Atmospheric Models for Air Quality Simulations in the Winter Season in China, Atmosphere, 17, 1,doi: 10.3390/atmos17010001, 2026.

Ng, N. L., Kwan, A. J., Surratt, J. D., Chan, A. W. H., Chhabra, P. S., Sorooshian, A., Pye, H. O. T., Crounse, J. D., Wennberg, P. O., Flagan, R. C., and Seinfeld, J. H.: Secondary organic aerosol (SOA) formation from reaction of isoprene with nitrate radicals (NO_3), Atmospheric Chemistry and Physics, 8, 4117-4140,doi: 10.5194/acp-8-4117-2008, 2008.

Otte, T. L. and Pleim, J. E.: The Meteorology-Chemistry Interface Processor (MCIP) for the CMAQ modeling system: updates through MCIPv3.4.1, Geosci. Model Dev., 3, 243-256,doi: http://10.5194/gmd-3-243-2010, 2010.

Place, B. K., Hutzell, W. T., Appel, K. W., Farrell, S., Valin, L., Murphy, B. N., Seltzer, K. M., Sarwar, G., Allen, C., Piletic, I. R., D'Ambro, E. L., Saunders, E., Simon, H., Torres-Vasquez, A., Pleim, J., Schwantes, R. H., Coggon, M. M., Xu, L., Stockwell, W. R., and Pye, H. O. T.: Sensitivity of northeastern US surface ozone predictions to the representation of atmospheric chemistry in the Community Regional Atmospheric Chemistry Multiphase Mechanism (CRACMMv1.0), Atmospheric Chemistry and Physics, 23, 9173-9190,doi: 10.5194/acp-23-9173-2023, 2023.

Pye, H. O. T., Luecken, D. J., Xu, L., Boyd, C. M., Ng, N. L., Baker, K. R., Ayres, B. R., Bash,

J. O., Baumann, K., Carter, W. P. L., Edgerton, E., Fry, J. L., Hutzell, W. T., Schwede, D. B., and Shepson, P. B.: Modeling the Current and Future Roles of Particulate Organic Nitrates in the Southeastern United States, Environmental Science & Technology, 49, 14195-14203,doi: 10.1021/acs.est.5b03738, 2015.

Pye, H. O. T., Pinder, R. W., Piletic, I. R., Xie, Y., Capps, S. L., Lin, Y.-H., Surratt, J. D., Zhang, Z., Gold, A., Luecken, D. J., Hutzell, W. T., Jaoui, M., Offenberg, J. H., Kleindienst, T. E., Lewandowski, M., and Edney, E. O.: Epoxide Pathways Improve Model Predictions of Isoprene Markers and Reveal Key Role of Acidity in Aerosol Formation, Environmental Science & Technology, 47, 11056-11064,doi: 10.1021/es402106h, 2013.

Pye, H. O. T., Place, B. K., Murphy, B. N., Seltzer, K. M., D'Ambro, E. L., Allen, C., Piletic, I. R., Farrell, S., Schwantes, R. H., Coggon, M. M., Saunders, E., Xu, L., Sarwar, G., Hutzell, W. T., Foley, K. M., Pouliot, G., Bash, J., and Stockwell, W. R.: Linking gas, particulate, and toxic endpoints to air emissions in the Community Regional Atmospheric Chemistry Multiphase Mechanism (CRACMM), Atmospheric Chemistry and Physics, 23, 5043-5099,doi: 10.5194/acp-23-5043-2023, 2023.

Sarwar, G., Luecken, D., Yarwood, G., Whitten, G. Z., Carter, W. P. J. J. o. a. m., and climatology: Impact of an updated carbon bond mechanism on predictions from the CMAQ modeling system: Preliminary assessment, 47, 3-14, 2008.

Seinfeld, J. H., Pandis, S. N. J. A. c., and physics: From air pollution to climate change, 1326, 1998.

Simon, H., Baker, K. R., and Phillips, S.: Compilation and interpretation of photochemical model performance statistics published between 2006 and 2012, Atmospheric Environment, 61, 124-139,doi: https://doi.org/10.1016/j.atmosenv.2012.07.012, 2012.

Skamarock, W. C., Klemp., J., Dudhia., J., Gill., D. O., Liu., Z., and Berner., J.: A Description of the Advanced Research WRF Model Version 4,doi: https://doi.org/10.5065/1dfh-6p97, 2019.

Skipper, T. N., D'Ambro, E. L., Wiser, F. C., McNeill, V. F., Schwantes, R. H., Henderson, B. H., Piletic, I. R., Baublitz, C. B., Bash, J. O., Whitehill, A. R., Valin, L. C., Mouat, A. P., Kaiser, J., Wolfe, G. M., St. Clair, J. M., Hanisco, T. F., Fried, A., Place, B. K., and Pye, H. O. T.: Role of chemical production and depositional losses on formaldehyde in the Community Regional Atmospheric Chemistry Multiphase Mechanism (CRACMM), Atmospheric Chemistry and Physics, 24, 12903-12924,doi: 10.5194/acp-24-12903-2024, 2024.

Stockwell, W. R., Lawson, C. V., Saunders, E., and Goliff, W. S.: A Review of Tropospheric Atmospheric Chemistry and Gas-Phase Chemical Mechanisms for Air Quality Modeling, Atmosphere, 3, 1-32,doi: 10.3390/atmos3010001, 2012.

Tsai, Y. G., Wang, J. Y., Yang, K. D., Yang, H. Y., Yeh, Y. P., Chang, Y. J., Lee, J. H., Wang, S. L., Huang, S. K., and Chan, C. C.: Long-term PM(2.5) exposure impairs lung growth and increases airway inflammation in Taiwanese school children, ERJ open research, 11,doi: 10.1183/23120541.00972-2024, 2025.

Wang, Y., Pavuluri, C. M., Fu, P., Li, P., Dong, Z., Xu, Z., Ren, H., Fan, Y., Li, L., Zhang, Y.-L., and Liu, C.-Q.: Characterization of Secondary Organic Aerosol Tracers over Tianjin, North China during Summer to Autumn, ACS Earth and Space Chemistry, 3, 2339-2352,doi: 10.1021/acsearthspacechem.9b00170, 2019.

Wong, D. C., Willison, J., Pleim, J. E., Sarwar, G., Beidler, J., Bullock, R., Herwehe, J. A., Gilliam, R., Kang, D., Hogrefe, C., Pouliot, G., and Foroutan, H.: Development of the MPAS-CMAQ coupled system (V1.0) for multiscale global air quality modeling, Geosci. Model Dev., 17, 7855-7866,doi: 10.5194/gmd-17-7855-2024, 2024.

Yarwood, G., Morris, R. E., and Wilson, G. M.: Particulate Matter Source Apportionment Technology (PSAT) in the CAMx Photochemical Grid Model, Air Pollution Modeling and Its Application XVII, Boston, MA, 2007//, 478-492,

Yarwood, G., Rao, S., Yocke, M., and Whitten, G.: Updates to the carbon bond chemical mechanism: CB05 final report to the US EPA, RT-0400675, 2005.

Zhang, J., He, X., Ding, X., Yu, J. Z., and Ying, Q.: Modeling Secondary Organic Aerosol Tracers and Tracer-to-SOA Ratios for Monoterpenes and Sesquiterpenes Using a Chemical Transport Model, Environmental Science & Technology, 56, 804-813,doi: 10.1021/acs.est.1c06373, 2022.

Zhang, J., He, X., Gao, Y., Zhu, S., Jing, S., Wang, H., Yu, J. Z., and Ying, Q.: Assessing Regional Model Predictions of Wintertime SOA from Aromatic Compounds and Monoterpenes with Precursor-specific Tracers, Aerosol and Air Quality Research, 21,doi: 10.4209/aaqr.210233, 2021.

Zhang, J., Liu, J., Ding, X., He, X., Zhang, T., Zheng, M., Choi, M., Isaacman-VanWertz, G., Yee, L., Zhang, H., Misztal, P., Goldstein, A. H., Guenther, A. B., Budisulistiorini, S. H., Surratt, J. D., Stone, E. A., Shrivastava, M., Wu, D., Yu, J. Z., and Ying, Q.: New formation and fate of Isoprene SOA markers revealed by field data-constrained modeling, npj Climate and Atmospheric Science, 6, 69,doi: 10.1038/s41612-023-00394-3, 2023.

Zhu, S., Wang, Z., Qu, K., Xu, J., Zhang, J., Yang, H., Wang, W., Sui, X., Wei, M., and Liu, H.: Spatial Characteristics and Influence of Topography and Synoptic Systems on PM2.5 in the Eastern Monsoon Region of China, Aerosol and Air Quality Research, 23, 220393,doi: 10.4209/aaqr.220393, 2023.